

Ultrathin Shape Change Smart Materials

Weinan Xu,¹ Kam Sang Kwok,¹ David H. Gracias^{1,2}

¹ Department of Chemical and Biomolecular Engineering, Johns Hopkins University, Baltimore, Maryland 21218, USA

² Department of Materials Science and Engineering, Johns Hopkins University, Baltimore, Maryland 21218, USA

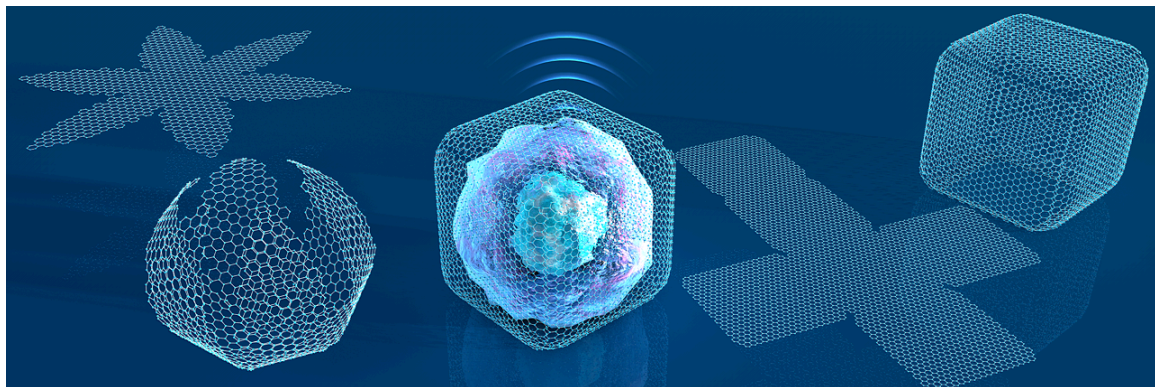
CONSPECTUS

With the discovery of graphene, significant research has focused on the synthesis, characterization, and applications of ultrathin materials. Graphene has also brought into focus broadly other ultrathin materials composed of organics, polymers, inorganics, and their hybrids. Together, these ultrathin materials have unique properties of broad significance. For example, ultrathin materials have a large surface area and high flexibility which can enhance conformal contact in wearables and sensors leading to improved sensitivity. When porous, the short transverse diffusion length in these materials allows rapid mass transport. Alternatively, when impermeable, these materials behave as an ultrathin barrier. Such controlled permeability is critical in the design of encapsulation and drug delivery systems. Finally, ultrathin materials often feature defect-free and single-crystal-like two-dimensional atomic structures resulting in superior mechanical, optical and electrical properties.

A unique property of ultrathin materials is their low bending rigidity, which suggests that they could easily be bent, curved or folded into 3D shapes. In this account, we review the emerging field of 2D to 3D shape transformations of ultrathin materials. We broadly define ultrathin to include films with a thickness of less than 100 nm and composed of a range of organic, inorganic and hybrid chemistries. This topic is important for both fundamental and applied reasons. Fundamentally, bending and curving of ultrathin films can cause atomistic and molecular strain which can alter their physical and chemical properties and lead to new 3D forms of matter which behave very differently from their planar precursors. Shape change can also lead to new 3D architectures with significantly smaller form factors. For example, 3D ultrathin materials would occupy a smaller space in on-chip devices or could permeate through tortuous media which is important for miniaturized robots and smart dust applications.

Our account highlights several differences between ultrathin and traditional shape change materials. The latter is typically associated with hydrogels, liquid crystals or shape memory elastomers. As compared to bulk materials, ultrathin films can much more easily bend and fold due to the significantly reduced bending modulus. Consequently, it takes much less energy to alter the shape of ultrathin materials and even small environmental stimuli can trigger a large response. Further, the energy barriers between different configurations are small which allows for a variety of conformations and enhances

programmability. Finally, due to their ultrathin nature, the shape changes are typically not slowed down by sluggish mass or thermal transport, and thus responses can be much faster than bulk materials. The latter point is important in the design of high-speed actuators. Consequently, ultrathin materials could enable low-power, rapid, programmable, and complex shape transformations in response to a broad range of stimuli such as pH, temperature, electromagnetic fields or chemical environments. The account also includes a discussion of applications, important challenges, and future directions.



1. INTRODUCTION

The history of ultrathin films can be dated back to the discovery of two-dimensional (2D) molecular films of fatty acids at the air-water interface by Langmuir in 1920s.¹ More recently, there has been a renaissance in research on ultrathin materials with the discovery of graphene.² It is now well-established that a decrease in the thickness of a material can significantly alter its physical and chemical properties, which is evident when comparing the properties of graphene and graphite. While a large focus has been devoted to elucidating the properties and applications of these materials in their planar 2D form, it has been recently suggested that the low bending rigidity of these films would allow them to be readily bent, curved and folded.³ Indeed, the bending or flexural rigidity (D) of a plate scales as $D \propto t^3$ where t is the thickness.⁴ This scaling with a strong dependence on thickness suggests that an ultrathin plate with a thickness of 1 nm is 1000 times easier to bend as compared to a plate with a thickness of 10 nm. Thus, shape changes in ultrathin materials driven by bending, curving and folding could be more readily achieved as compared to thicker or bulk materials.

In this account, we discuss research on shape changes of ultrathin materials. To broaden the scope, we discuss materials whose thickness (shell thickness for hollow structures) is less than 100 nm, and include a wide range of material compositions including organics, polymers, inorganics, and their hybrids. We note that our account excludes conventional shape change smart materials with a thickness greater than 100 nm as well as bulk materials such as responsive hydrogels,⁵ shape memory elastomers,⁶ liquid crystal elastomers,⁷ and polymer nanocomposites.⁸ Readers with an interest in shape changes of thicker materials are directed to several comprehensive reviews.^{9,10}

There are several important differences between the shape change of bulk and ultrathin materials. Firstly, due to the low bending rigidity of ultrathin materials, the energy required to bend, curve or fold them is much lower than thicker materials, and consequently stimuli-responsive 2D to 3D shape change can be triggered occur under milder conditions. This point is important from the practical standpoint of facilitating low-power actuation and operation of shape change devices. In addition, small energetic barriers for folding suggest that a variety of 3D conformations could be realized. Secondly, due to their ultrathin nature, mass and thermal transport barriers that often delay shape changes in bulk materials are less of a concern. For example, the time scale for shape change of bulk hydrogels such as poly(N-isopropylacrylamide) (PNIPAM) is limited by water diffusion and thermal transport, both of which are thickness dependent. It is envisioned that shape change of ultrathin materials could thus be enabled at much faster time scales as compared to bulk materials. Finally, when combined with shape transformation from 2D to 3D, the inherent excellent properties of ultrathin materials such as their lightweight, large surface area and low defects could enable high performance and small form factor devices with unprecedented functionalities. It is noteworthy here, that the volume occupied by a 1 nm thick film with a lateral dimension of 1 x 1 cm is approximately the same as that of a 3D object with 50 μ m in size, or the size of a biological cell. Hence, it is conceivable that the 2D to 3D shape transformation of ultrathin materials could dramatically shrink their size which is of importance in dispersible sensors, smart dust, and miniaturized robots. In addition, the flexibility and large surface area provide an ideal substrate for conformal contact in shell sensors.¹¹

In this account, we review the recent progress in ultrathin shape change materials and categorize them based on their composition and the mechanism that triggers shape change (Table 1). We discuss the unique properties and promising applications of ultrathin shape change materials in electronics, optics, and biomedicine. Finally, challenges and future directions are outlined

Table 1. Major categories of ultrathin shape change materials and their characteristics.

Category	Material composition	Lateral Size	Thickness	Shape change mechanism	Refs
liposomes/ lipid vesicles	lipids	20 nm to 10 μ m	<5 nm	biological stimuli, such as proteins, lipoproteins	12,13
micelles/ polymersomes	amphiphilic polymers	10 nm to 10 μ m	5-20 nm	pH, temperature, light, magnetic fields, chemical signals	14,15
polymer platelets/thin films	amphiphilic polymers/ polyelectrolytes	500 nm to mm	5-50 nm	pH, light, temperature	16,17
thin shell microcapsules	polyelectrolytes	500 nm to 10 μ m	10-50 nm	pH, temperature	18,19
inorganic membranes	metal, semiconductor, ceramics	100 nm to 10 μ m	3-50 nm	heat, ion beams, oxidation, residual stress	20,21
hybrid thin films	metal, 2D materials, nanoparticles, polymers	10-500 μ m	5-100 nm	temperature, salt, solvents, DNA	22,23

2. ULTRATHIN SHAPE CHANGE STRUCTURES COMPOSED OF ORGANICS

The morphological plasticity of biological membranes is critical for cellular physiological functions, as cells need to rearrange their membranes quickly during their life cycle. Lipids, by their ability to exist in many shapes (polymorphism), provide a superlative construction material for cellular membranes.²⁴ Supported lipid bilayers are

useful *in-vitro* mimics of natural biological membranes and can be used to model cell-cell interactions.

The fundamental processes of vesicle fusion and rupture in supported bilayers

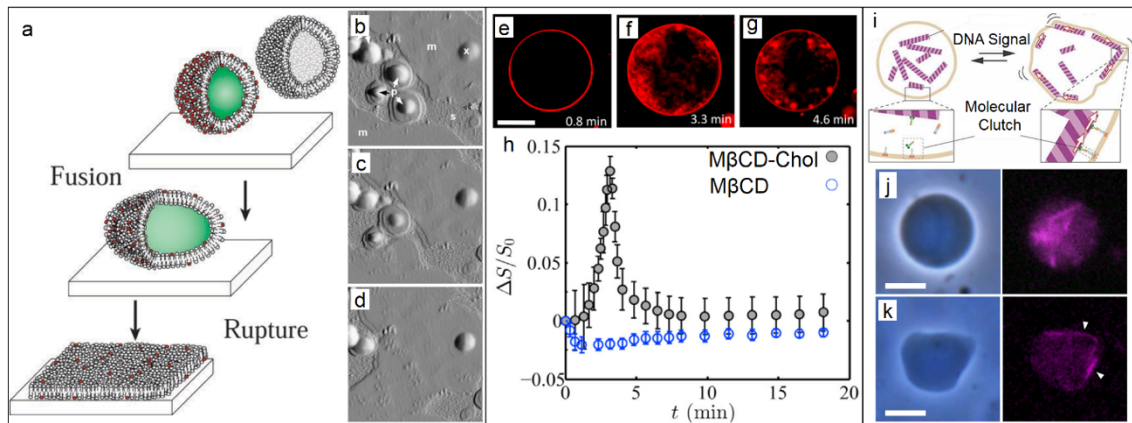


Figure 1. Ultrathin shape change structures based on lipids. (a) Schematic of the formation of a supported lipid bilayer. (b-d) Sequential AFM images demonstrating vesicle rupture and supported lipid bilayer formation on silica. All image sizes are $1.67 \times 1.67 \mu\text{m}$ (reproduced with permission from refs 12 and 13; copyright 2000 and 2002 Elsevier Inc.). (e-g) Confocal images show the response of liposomes to cholesterol with associated shape changes. Scale bar is $20 \mu\text{m}$. (h) Plot of the changes in the surface area of the liposomes with time (reproduced with permission from ref 25; copyright 2016 Elsevier Inc.). (i) Schematic of lipid robots in inactive and active states. (j-k) Phase-contrast microscopy images of lipid robots and fluorescence images of microtubules in, (j) inactive, and (k) active states. Scale bars are $10 \mu\text{m}$ (reproduced with permission from ref 26; copyright 2017 American Association for the Advancement of Science).

which involves mixing of lipids, as well as loss of encapsulated content, is depicted in Figure 1a.¹² This shape change process in a liquid environment is shown in Figure 1b-d.¹³ The lipid vesicles spread and flatten from the outer edges toward the center until the two bilayers stack on top of each other. Then, the top bilayer either rolls or slides over the bottom layer and the edges fuse together to form bigger patches.

The changes in the shape of cellular lipid bilayers are linked to critical physiological functions. For example, an increase of cholesterol in the plasma membrane increases the risk of atherosclerosis. This phenomenon is related to the cholesterol-induced shape

changes of liposomes, as shown in Figure 1e-h.²⁵ When exposed to a high concentration of cholesterol, the liposomes initially respond with an increase in their surface area and membrane fluctuations. At later times, the liposome surface area decreases, as demonstrated by the decrease in the vesicle perimeter and the shrinkage of tubes into intra-vesicle buds.

Dynamical processes in the shape change of lipid vesicles can be thought of as complex motions of machines. In fact, an amoeba-like molecular robot which can express continuous shape changes in response to specific signal molecules has been reported (Figure 1i).²⁶ The body of the robot is a lipid vesicle; the actuator driving the shape changes is composed of proteins, kinesin, and microtubules. The robot exhibits continuous changes in shape when actuated with a sequence-designed DNA molecule (Figure 1j-k), and the shape change behavior is terminated with the triggered release of the signal DNA molecule.

3. ULTRATHIN SHAPE CHANGE STRUCTURES COMPOSED OF POLYMERS

3.1 Shape change micelles and polymersomes

Amphiphilic responsive polymers can self-assemble into micelles or polymersomes with an ultrathin shell in selective solvents. For micelles and polymersomes made from thermoresponsive polymers, a temperature change can induce shrinkage, fusion or reorganization. For instance, triblock copolymers with a temperature responsive PNIPAM block have been synthesized.¹⁴ They self-assemble into spherical micelles at room temperature (Figure 2a-d) and undergo sphere-to-cylinder shape changes above the lower critical solution temperature (LCST) due to a conformational

change of PNIPAM. The reversible cylinder-to-sphere transition occurs when the temperature is decreased below the LCST.

The physical and chemical interactions between macromolecules, e.g., hydrogen bonding or chemical bonding, can also be utilized to achieve shape changes. For instance,

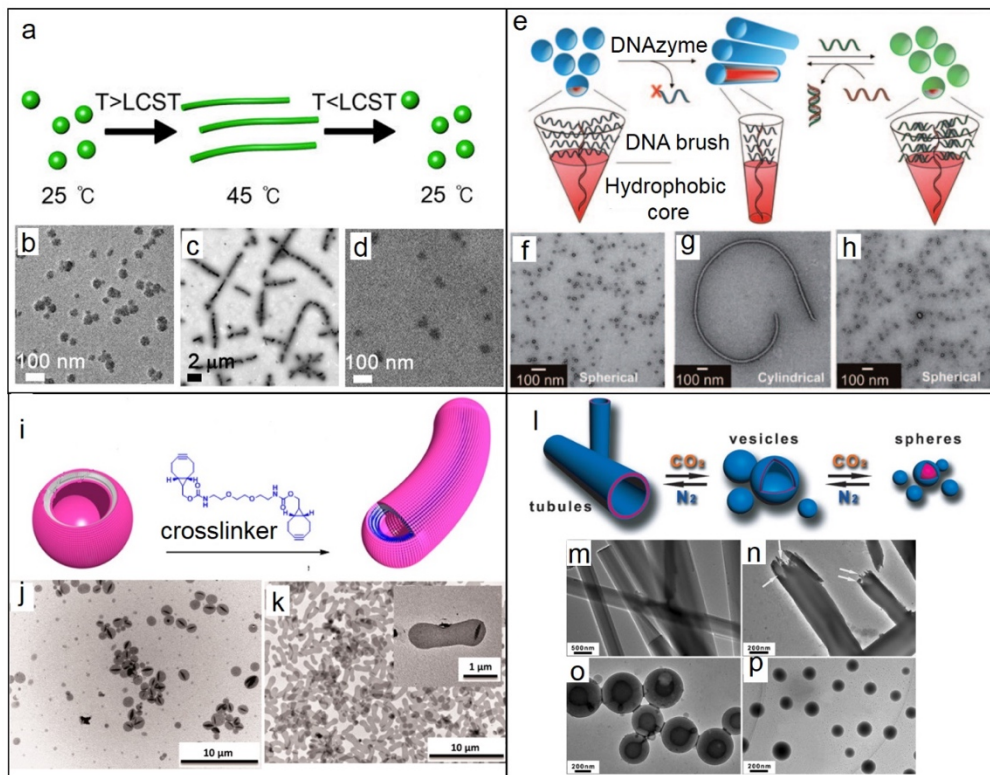


Figure 2. Shape change of ultrathin micelles and polymersomes. (a-d) Temperature induced shape change and recovery of the micelles. TEM images of the micelles at, (b) 25 °C, (c) 45 °C and, (d) cool down to 25 °C (reproduced with permission from ref 14; copyright 2016 American Chemical Society). (e) Shape change of micelles self-assembled from of DNA-brush copolymers. (f-h) TEM images of, (f) spherical micelles, (g) cylindrical micelles after addition of DNAzyme, and (h) spherical micelles after addition of complementary ssDNA (reproduced with permission from ref 15; copyright 2010 Wiley-VCH). (i) Shape transformation of polymersomes induced by a crosslinker. (j-k) TEM images of polymersomes after adding increasing amounts of crosslinker molecules (reproduced from ref 27; copyright 2013 American Chemical Society). (l) Schematic of the CO₂-driven shape transformation. TEM images of the assembled structures in different levels of CO₂ stimulus: (m, n) no stimulus, (o) 15 min, (p) 25 min (reproduced with permission from ref 28; copyright 2013 Wiley-VCH).

when DNA strands are introduced to amphiphilic block copolymers, the shape of the self-assembled micelles can be manipulated by sequence-selective interactions, which dominate steric and electrostatic repulsions. In one example, DNA-brush copolymer

amphiphiles assemble into spherical micelles (Figure 2e-h).¹⁵ To facilitate a sphere-to-cylinder phase transition, the spherical micelles are mixed with a DNA based phosphodiesterase, which is able to recognize a given DNA sequence and cut it at a designated position. This process results in a truncated DNA sequence, and subsequent reorganization to cylindrical micelles. Moreover, the opposite process: cylinder-to-sphere phase transition, can be achieved by adding an input DNA sequence, which forms a duplex with the truncated DNA in the cylindrical shell, and the bulky, extended duplex is better accommodated in the spherical micellar phase.

Chemical crosslinking has also been shown to induce the shape change of ultrathin polymeric structures. For instance, amphiphilic block copolymers poly(ethylene glycol)-*b*-poly(styrene-*co*-4-vinylbenzyl azide) self-assemble into spherical polymersomes in a selective solvent (Figure 2i-k).²⁷ Due to the existence of azide functional groups on the polymer, when excess crosslinkers with alkyne groups are added to the solution, a strain-promoted cycloaddition reaction happens, which induces the polymersomes to stretch in one dimension into a tubular shape upto 2 μ m in length. The asymmetry in the crosslinking density of the membrane is the main reason for the spontaneous curvature and shape transformation.

Small gas molecules can also be used to induce shape change of ultrathin polymeric assemblies. For instance, amidine-containing block copolymers, which consist of poly((*N*-amidine) dodecylacrylamide) as the intermediate CO₂-sensitive block, self-assemble into microscopic tubular architectures in aqueous solutions (Figure 2l-p).²⁸ By introducing CO₂ gas into this system, the middle block is gradually protonated by the acidic gaseous medium. The alteration in amphiphilicity drives the reshaping of the

tubular structure to spherical vesicles. Further extended exposure to CO₂ leads to the transformation of vesicles to spherical micelles. Methods to induce shape changes of responsive micelles and polymersomes are not limited to those discussed above. Alternate stimuli can be used which include pH, light, electrical or magnetic fields, and redox reactions.^{29,30} The capacity of such systems to exhibit a variety of shape adaptations in response to a range of stimuli is critical for their use in advanced drug delivery and bioimaging.³¹

3.2 Shape change ultrathin polymer platelets or films

When responsive polymers are assembled in 2D space, they can form ultrathin platelets or films which can change their shape or size when exposed to specific stimuli. For instance, the crystallization-driven self-assembly of poly(ϵ -caprolactone)-*b*-poly(acrylic acid) (PCL-*b*-PAA) block copolymers results in ultrathin (sub-5 nm) Janus nanoplates,¹⁶ which are composed of partially cross-linked PAA and tethered PCL brush layers (Figure 3a). In an acidic environment, the carboxylic acid groups of PAA are protonated, inducing the PAA layer to contract; the Janus assembly, therefore, bends toward the PAA layer (Figure 3b-d). On the other hand, the PAA layer swells at pH 11 due to deprotonation, and the nanoplate bends toward the PCL layer. This reversible shape change is achieved by a remarkably small stress – about five orders of magnitude smaller than that needed for shape changes of conventional thick hydrogel bilayers.

Macroscopic ultrathin polymer films with pH-responsive properties, under confinement or within bounded templates, can also have ordered wrinkling/folding behaviors upon pH changes.³² For instance, exposure of a crosslinked poly-2-vinyl pyridine (P2VP) film (thickness: 20-100 nm) to acidic pH results in the transformation of

the initially smooth morphology into a network of anisotropic structures, the dimensions of which are governed by the thickness of the film (Figure 3e-f).¹⁷ When the ultrathin film is patterned into a well-ordered array, it deforms into well-defined curved structures upon

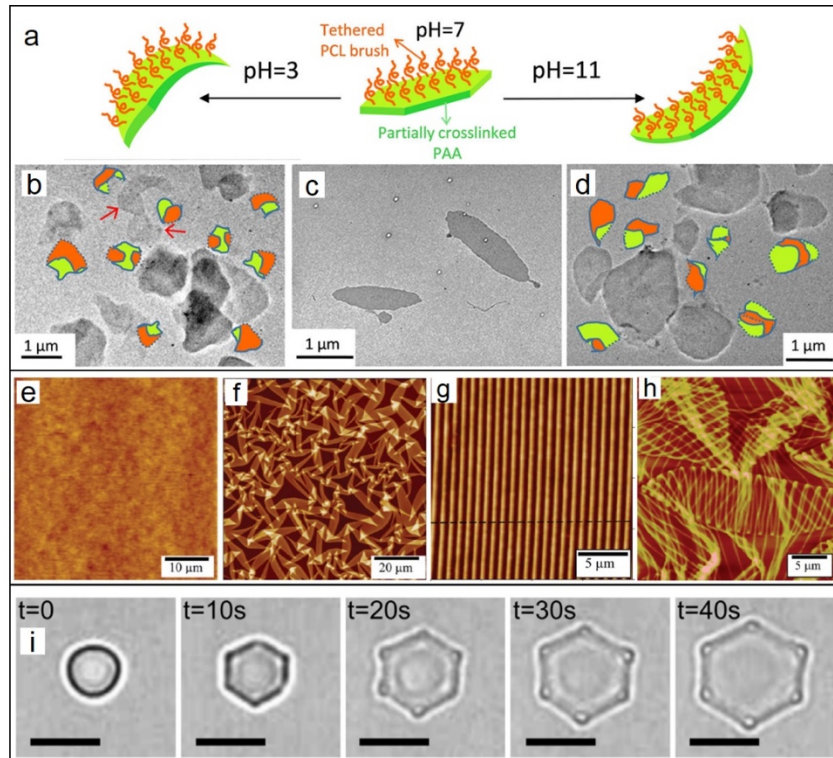


Figure 3. Ultrathin change change polymer platelet/film. (a) The shape change of a Janus PCL-b-PAA nanoplate at various pH. (b-d) TEM images of the Janus nanoplates at (b) pH 3, (c) pH 7, and (d) pH 11 (reproduced with permission from ref 16; copyright 2016 American Chemical Society). (e) AFM image of the pristine P2VP thin film, (f) the self-folded P2VP film upon exposure to acidic pH. (g) AFM images of nanostripe patterned P2VP thin film, and (h) the corresponding folded structures when exposed to acidic pH (reproduced with permission from ref 17; copyright 2010 American Chemical Society). (i) Optical microscopy images showing blue light-induced transformation of a single trans-azoTAB:PAA particle into a hexagonal platelet; scale bars are 5 μm (reproduced with permission from ref 34; copyright 2017 Nature Publishing Group).

pH variation (Figure 3g-h). The confinement of these ultrathin gel films caused by strong adhesion to the substrate and a high degree of swelling of the loosely crosslinked film on top are responsible for inducing the unique folding patterns.

Light-induced shape changes can be achieved by incorporating optically responsive polymers or functional groups.³³ For instance, micrometer-sized hydrated

particles based on the electrostatically co-assembly of PAA and trans-azobenzene trimethylammonium bromide (trans-azoTAB) have been reported (Figure 3i).³⁴ The trans-azoTAB:PAA irregular particle rapidly transforms into a hexagonal platelet under blue light illumination. Such photo-induced shape transition has been attributed to softening and fluidization of the hydrated polyelectrolyte-surfactant matrix during transformation to the photostationary trans/cis state, which in turn facilitates re-organization of the randomly aligned mesostructures into hexagonal platelets.

3.3. Shape change microcapsules with an ultrathin shell

Microcapsules with an ultrathin shell can be fabricated using layer-by-layer (LbL) assembly on a sacrificial template. If the shell is composed of responsive polymers, the hollow 3D structures have the capability to change their shapes or sizes under certain conditions. For instance, poly(methacrylic acid) (PMAA) cubic microcapsules bulge into a spherical shape when pH is changed from acidic to basic, while capsule size remains virtually unchanged (Figure 4a-c).¹⁸

Moreover, the chemical composition and mechanical properties of the shell have a significant effect on the shape change of microcapsules. For instance, when two-component (PMAA–PV Pon)₅ (PV Pon: poly(*N*-vinylpyrrolidone)) microcapsules are exposed to basic pH (pH=8),¹⁹ they retain their cubic shapes while increasing in size by 40% (Figure 4d-e). These different shape responses have been rationalized by a difference in the shell rigidity expressed as the ratio of the polymer contour length between neighboring crosslinking points to the persistence polymer length. This analysis indicates that the two-component system is much more rigid.

pH-induced shape transformations have also been observed with anisotropic ultrathin capsules with high aspect ratio. For instance, discoidal PMAA capsules which mimic the shape of a red blood cell,³⁵ show a dramatic volume increase of 24-fold when exposed to basic pH (Figure 4f-g). The pH-triggered change in capsule dimensions also

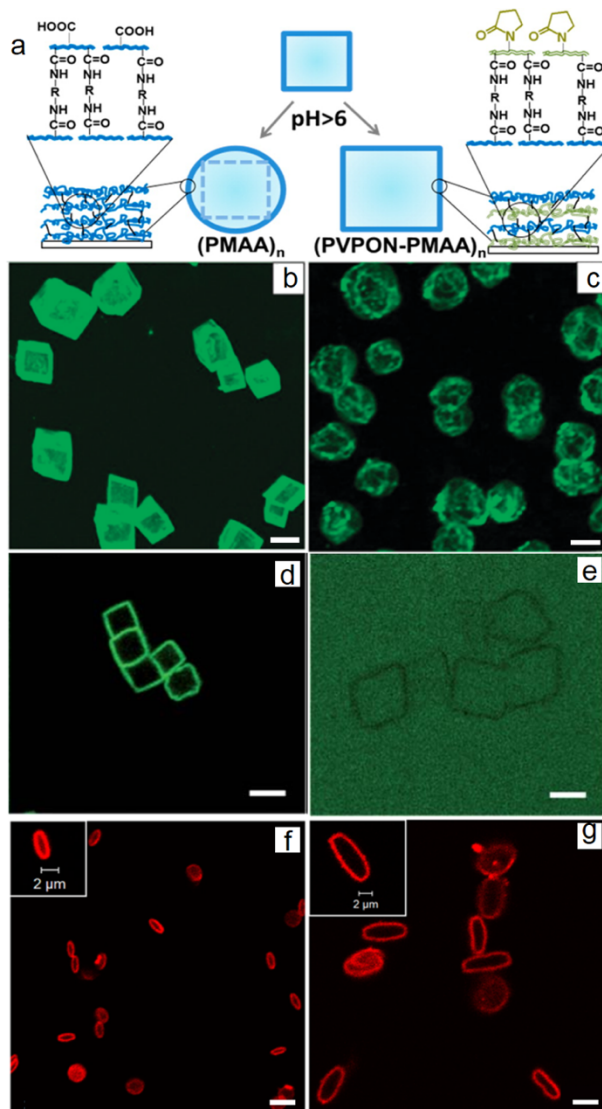


Figure 4. Shape change microcapsules with an ultrathin shell. (a) pH-triggered shape responses of single- and two-component cubic ultrathin shell capsules. (b-e) Confocal microscopy images of cubic hydrogel capsules (b-c) $(\text{PMAA})_{20}$, and (d-e) $(\text{PMAA-PVPON})_5$ when the solution pH was changed from 5 to 8 (Reproduced with permission from refs 18 and 19; copyright 2011 and 2012 Royal Society of Chemistry). Confocal microscopy images of discoidal $(\text{PMAA})_{15}$ ultrathin shell capsules at (f) pH 4 and (g) pH 7.4. All scale bars are 4 μm (Reproduced with permission from ref 35; copyright 2016 American Chemical Society).

results in anisotropic swelling/shrinkage leading to discoidal-to-ellipsoidal shape transformations where the extent of the shape transition depends on the shell composition.

To theoretically rationalize the shape change mechanisms of ultrathin soft matter systems discussed in the above sections, traditional continuum mechanics modeling which works well with bulk shape change materials, are usually not applicable because of the atomic level precision required as well as the ultrathin, irregular and porous nature of these structures.³⁶ Therefore, multiscale simulations based on coarse-grained molecular dynamics (MD) or dissipative particle dynamics (DPD) are necessary for modeling ultrathin systems.³⁷

4. ULTRATHIN SHAPE CHANGE STRUCTURES COMPOSED OF INORGANICS

Inorganic materials such as metals, semiconductors or ceramics are generally considered rigid, and not as easy to bend or fold as compared to organic materials. However, when their thickness is reduced to the nanometer scale, their bending rigidity is substantially decreased, and a large variety of 3D folded structures can be generated. For instance, ultrathin metal oxide nanosheets composed of MoO₃ (with thickness around 3.3 nm) could be gradually transformed into tubular multi-walled nanotubes in the presence of oxidant and oleylamine (Figure 5a-b).³⁸ Elsewhere, by reducing the thickness of nanocrystalline (NC) diamond membranes to 40 nm, their self-folding into 3D structures after release from the substrate due to an intrinsic stress gradient has been reported (Figure 5c).²⁰ The curvature of these folded structures can be tuned by changing the thickness and built-in strain of the nanomembranes.³⁹

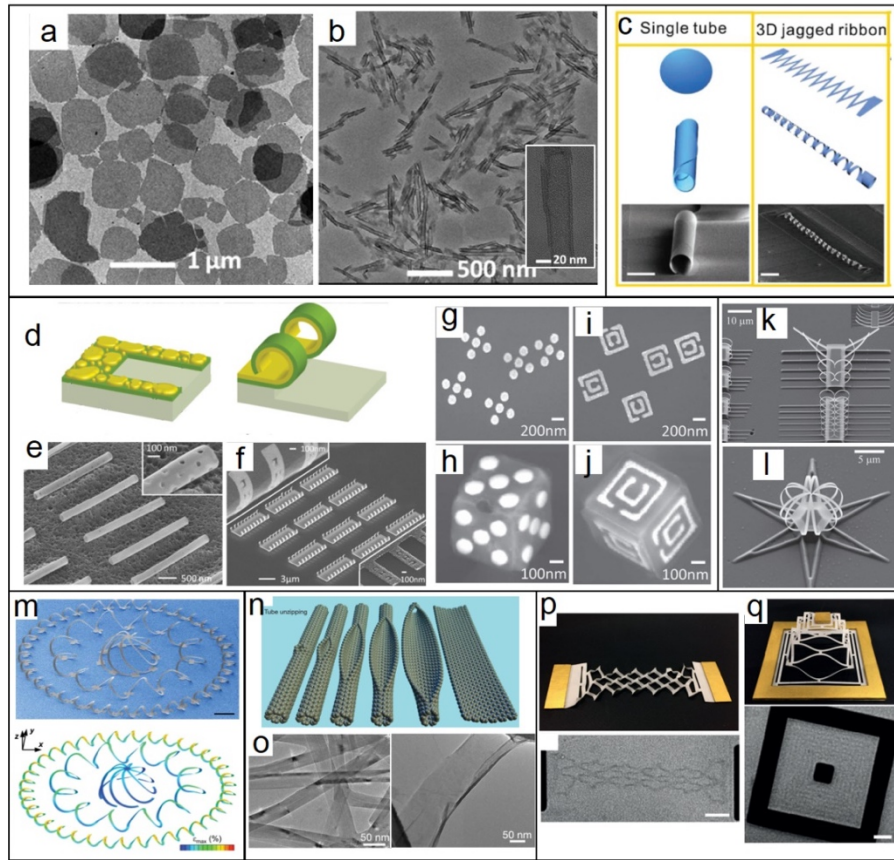


Figure 5. Shape change ultrathin inorganic materials. TEM image of, (a) ultrathin MoO_3 nanosheets, and (b) rolled-up multiwalled nanotubes (reproduced with permission from ref 38; copyright 2012 Wiley-VCH). (c-d) Schematics and SEM images of folded diamond nanomembranes, scale bars: 10 μm . (reproduced with permission from ref 20; copyright 2017 Wiley-VCH) (e-f) SEM images of shape change of ultrathin e-beam patterned Sn/Ni bilayer films (reproduced with permission from ref 21; copyright 2010 Wiley-VCH). (g-j) SEM images of e-beam patterned self-folded Al_2O_3 nanocubes (reproduced with permission from ref 40; copyright 2011 Wiley-VCH). SEM images of (k) self-rolling strips, and (l) flower shape formed from ultrathin Ti/Al/Cr films (reproduced with permission from ref 42; copyright 2013 Wiley-VCH). (m) SEM images and FEA predictions of a complex 3D mesostructure formed from a 2D precursor. Scale bar is 400 μm (reproduced with permission from ref 43; copyright 2015 American Association for the Advancement of Science). (n) The gradual unzipping of a carbon nanotube wall to form a nanoribbon. (o) TEM images depicting the transformation of MWCNTs (left) into oxidized nanoribbons (right) (reproduced with permission from ref 44; copyright 2009 Nature Publishing Group). (p-q) Paper model and graphene folding in the shape of, (p) in-plane kirigami springs, and (q) kirigami pyramid (reproduced with permission from ref 3; copyright 2015 Nature Publishing Group).

Surface forces generated by heat induced grain coalescence of ultrathin metal films can also be used to induce self-folding. For instance, tin (Sn) has been used as an

active material for self-folding, because of its low melting temperature.²¹ When a bilayer is formed with Sn and another thin metal or oxide layer (such as Ni, SiO₂, or Al₂O₃), the extrinsic stress upon Sn reflow leads to spontaneous curving and shape changes (Figure 5d-f). When combined with e-beam lithography, 3D curved and folded structures with a wide range of sizes, shapes and patterns can be generated. (Figure 5g-j).⁴⁰ In-situ processing techniques such as reactive ion etching (RIE) and focused ion beam (FIB) induced deformation can also be utilized to fold freestanding ultrathin films into complex 3D structures.⁴¹ For instance, FIB using high energy gallium ions generates stress by the generation of dislocations and ion implantation within material layers, which induces creases or folds upon mechanical relaxation (Figure 5k-l).⁴²

The shape transformation of ultrathin inorganic materials can also be achieved by extension and strain relaxation of the underlying substrate. For example, strain relaxation in an elastomeric substrate can simultaneously impart forces at a collection of pre-defined locations on the surfaces of planar precursor structures (Figure 5m).⁴³ The resulting processes of controlled, compressive buckling induce rapid, large-area geometric extension into the third dimension, capable of transforming advanced functional materials and planar microsystems into mechanically tunable 3D forms with broad geometric variations.

Atomically ultrathin 2D materials such as graphene also have the potential to change their shape or dimension triggered by chemical reaction or external mechanical force. An extreme example is the unzipping of carbon nanotubes (CNT) which leads to graphene nanoribbons (Figure 5n-o).⁴⁴ Shape transformation of graphene can also be achieved using mechanical forces and this approach has been utilized to enable

graphene kirigami and construct mechanical metamaterials such as stretchable electrodes, springs, and hinges (Figure 5p-q).³

5. ULTRATHIN SHAPE CHANGE STRUCTURES COMPOSED OF HYBRIDS

It is often feasible and desirable to combine organic and inorganic materials to fabricate hybrid ultrathin materials that have shape-change capabilities. In this way, the final structures have the potential to incorporate the advantageous properties of both material classes. For instance, a thermally responsive method to fold and unfold monolayer graphene into predesigned, ordered 3D structures has been recently developed.²² The methodology involves the non-covalent surface functionalization of graphene with polydopamine and thermoresponsive PNIPAM brushes (Figure 6a). The functionalized graphene is micropatterned and self-folds into ordered 3D structures with reversible deformation under full control by temperature (Figure 6b-d). A multiscale theoretical model was developed and used to design ordered 3D graphene structures with predictable shape and dynamic. The ultrathin graphene-organic hybrids show reversible actuation and can encapsulate live cells; the controlled folding can be used to also fabricate non-linear resistor and creased transistor devices.

Ultrathin bilayers composed of metal and polymer hybrids have been reported. For instance, ultrathin Au–polymer brush composite objects have been fabricated by microcontact printing followed by brush growth and etching of the substrate.⁴⁵ These objects fold into 3D microstructures in response to different solvents that can change the conformation or swelling of the polymer brushes (Figure 6e-h). The bending of these objects can be predicted, and hence predefined during the synthesis process by controlling the dimensions of the gold layer and the polymer brush.

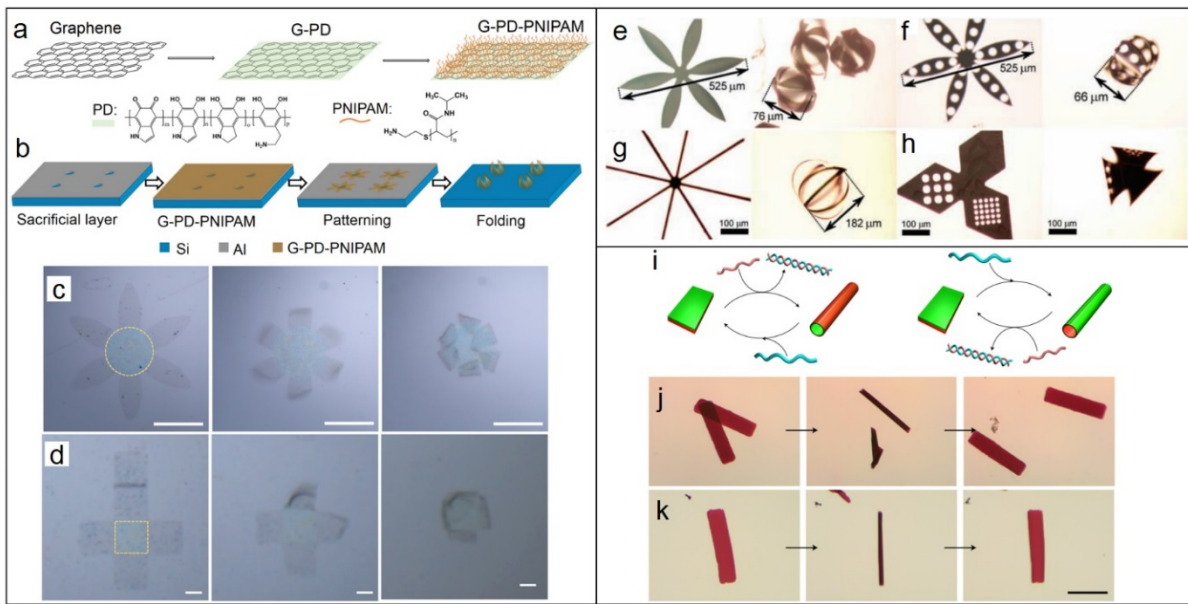


Figure 6. Organic / Inorganic hybrid shape change ultrathin materials. (a) Schematic illustration of the surface functionalization process of graphene. (b) The fabrication and folding process of ultrathin graphene-polymer brush hybrids. (c-d) Optical microscope snapshots of the self-folding of ultrathin graphene microstructures after heating to 45 °C. Scale bars are 100 μm (reproduced with permission from ref 22; copyright 2017 American Association for the Advancement of Science). (e-h) Au-polymer brush bilayer structures in the flat (left) and folded (right) state (reproduced with permission from ref 45; copyright 2011 Wiley-VCH). (i) Schematics of the programmed actuation of DNA-GNP films. (j-k) Corresponding microscope images of the processes. Scale bar is 200 μm (reproduced with permission from ref 23; copyright 2017 Nature Publishing Group).

In another recent example, shape change films composed DNA and gold nanoparticles have been reported.²³ The films are formed from DNA-grafted gold nanoparticles using a LbL deposition process. Films consisting of an active and a passive layer show rapid, reversible curling in response to complementary stimulus DNA strands added to the solution (Figure 6i-k). The researchers attribute the shape change mechanism to the addition of filler DNA strands and exchange reactions which lead to an increase in the interparticle distance, and cause swelling of the active layer; the strain mismatch between the swollen active and non-swollen passive layer curls the film.

6. SUMMARY AND OUTLOOK

Ultrathin shape change structures can be created with a wide range of organic, polymeric, inorganic and hybrid components. Further, their sizes and dimensions also span a wide range of shapes and sizes. As discussed, ultrathin shape change materials are distinct from their bulk counterparts, such as hydrogel or elastomers.⁴⁶ In contrast to conventional bulk materials synthesis and processing, the fabrication of ultrathin shape change structures often requires either controlled molecular self-assembly at the nanometer scale or top-down nanopatterning techniques. For instance, stimuli-responsive micelles or polymersomes are generally formed by the self-assembly of amphiphilic block copolymers; the self-rolling inorganic nanotubes are fabricated by physical vapor deposition and photo/e-beam lithography. Since the energy barriers for bending are lower than bulk materials, forces required to fold these ultrathin films are significantly lower, and thus conditions for shape changes are often much milder. Typically, a slight increase in temperature or a small variation in pH is enough to cause shape changes. Consequently, there are more varieties in the possible shape-change mechanisms for ultrathin structures, and even DNA hybridization, gas adsorption or chemical reactions could induce changes in the shape of these materials. Finally, the response of such ultrathin shape change materials is much faster than their bulk counterparts especially when mass or heat transport is involved.

The broad applications of ultrathin shape change materials span from flexible and wearable electronics to drug delivery and biosensing. Illustrative examples of applications include a 3D photodetector with a rolled-up geometry which exhibits broadband enhancement of coupling efficiency and omnidirectional detection under a wide incident

angle compared with its 2D counterpart.⁴⁷ In drug delivery applications, pH-responsive polymersomes can efficiently encapsulate and release drug/DNA molecules to specific locations in the body with temporal control.⁴⁸ Self-folding microgrippers can be used to enable untethered biopsies, capture single cells and enable 3D analysis of cell membranes.¹¹

Apart from the exciting progress in ultrathin shape change materials achieved so far, there are significant challenges that need to be overcome. For ultrathin structures fabricated with lithographic techniques, it is challenging to scale up fabrication and generate, for example, gram quantities in a cost-effective manner. The uniformity and monodispersity of self-assembled ultrathin shape change structures need to be improved. Additionally, the stability of the ultrathin shape change materials is limited. Especially, the stability of 3D hollow structures with ultrathin shells is strongly dependent on the environment. For instance, responsive polymersomes or microcapsules, are only stable in liquids and collapse upon drying, techniques such as critical point drying are necessary to maintain their 3D shapes in the dry state. Finally, the rational design of these structures requires the development of advanced multiscale modeling to bridge atomistic and larger continuum length scales.²²

Nonetheless, with the rapid development of 2D nanomaterials, surface chemistry, and nanofabrication, we expect new approaches to be realized in the rational design, fabrication, and characterization of ultrathin shape change materials. We anticipate that the combination of 2D layered materials, supramolecular chemistry, and responsive polymers will generate many new and unprecedented functional shape change structures.

AUTHOR INFORMATION

Corresponding Author

*E-mail: dgracias@jhu.edu

Notes

The authors declare no competing financial interest.

Biographical Information

Weinan Xu received his Ph.D. from Georgia Institute of Technology in 2015. He is currently a postdoctoral fellow at the Johns Hopkins University working on ultrathin 3D structures based on 2D nanomaterials.

Kam Sang Kwok received his B.S. from the University of Illinois at Urbana-Champaign in 2013; he is currently a Ph.D. student at the Johns Hopkins University working on manufacturing 3D nanostructures.

David H. Gracias is a Professor at the Johns Hopkins University. He received his Ph.D. from the University of California at Berkeley in 1999 and did post-doctoral work at Harvard University, all in chemistry or related fields. His independent laboratory, since 2003, has pioneered the development of 3D, integrated micro and nanodevices using a variety of patterning, self-folding, and self-assembly approaches. Prof. Gracias has co-authored over 150 technical publications and is a co-inventor of 30 issued patents.

ACKNOWLEDGEMENTS

This work was supported by the Air Force Office of Scientific Research MURI program (FA9550-16-1-0031) and the National Science Foundation CMMI-1635443.

REFERENCES

- 1 Langmuir, I. The Mechanism of the Surface Phenomena of Flotation. *Trans. Faraday Soc.* **1920**, *15*, 62-74.
- 2 Novoselov, K. S.; Mishchenko, A.; Carvalho, A.; Neto, A. C. 2D Materials and van der Waals Heterostructures. *Science* **2016**, *353*, aac9439.
- 3 Blees, M. K.; Barnard, A. W.; Rose, P. A.; Roberts, S. P.; McGill, K. L.; Huang, P. Y.; Ruyack, A. R.; Kevek, J. W.; Kobrin, B.; Muller, D. A.; McEuen, P. L. Graphene Kirigami. *Nature* **2015**, *524*, 204-207.
- 4 Landau, L. D.; Lifshitz, E. M. Course of Theoretical Physics, Theory of Elasticity, Pergamon Press, London, 3rd Ed, vol. 7, 1986.
- 5 Hu, X.; Zhou, J.; Vatankhah-Varnosfaderani, M.; Daniel, W. F.; Li, Q.; Zhushma, A. P.; Dobrynin, A. V.; Sheiko, S. S. Programming Temporal Shapeshifting. *Nat. Commun.* **2016**, *7*, 12919.
- 6 Zhao, Q.; Qi, H. J.; Xie, T. Recent Progress in Shape Memory Polymer: New Behavior, Enabling Materials, and Mechanistic Understanding. *Prog. Polym. Sci.* **2015**, *49*, 79-120.
- 7 Ware, T. H.; McConney, M. E.; Wie, J. J.; Tondiglia, V. P.; White, T. J. Voxelated Liquid Crystal Elastomers. *Science* **2015**, *347*, 982-984.
- 8 Gladman, A. S.; Matsumoto, E. A.; Nuzzo, R. G.; Mahadevan, L.; Lewis, J. A. Biomimetic 4D Printing. *Nat. Mater.* **2016**, *15*, 413-418.
- 9 Jeon, S. J.; Hauser, A. W.; Hayward, R. C. Shape-Morphing Materials from Stimuli-Responsive Hydrogel Hybrids. *Acc. Chem. Res.* **2017**, *50*, 161-169.
- 10 Ko, H.; Javey, A. Smart Actuators and Adhesives for Reconfigurable Matter. *Acc. Chem. Res.* **2017**, *50*, 691-702.
- 11 Jin, Q.; Li, M.; Polat, B.; Paidi, S. K.; Dai, A.; Zhang, A.; Pagaduan, J. V.; Barman, I.; Gracias, D. H. Mechanical Trap Surface-Enhanced Raman Spectroscopy for Three-Dimensional Surface Molecular Imaging of Single Live Cells. *Angew. Chem. Int. Ed.* **2017**, *129*, 3880-3884.
- 12 Johnson, J. M.; Ha, T.; Chu, S.; Boxer, S. G. Early Steps of Supported Bilayer Formation Probed by Single Vesicle Fluorescence Assays. *Biophys. J.* **2002**, *83*, 3371-3379.
- 13 Jass, J.; Tjärnhage, T.; Puu, G. From Liposomes to Supported, Planar Bilayer Structures on Hydrophilic and Hydrophobic Surfaces: An Atomic Force Microscopy Study. *Biophys. J.* **2000**, *79*, 3153-3163.
- 14 Kim, C. J.; Hu, X.; Park, S. J. Multimodal Shape Transformation of Dual-Responsive DNA Block Copolymers. *J. Am. Chem. Soc.* **2016**, *138*, 14941-14947.
- 15 Chien, M. P.; Rush, A. M.; Thompson, M. P.; Gianneschi, N. C. Programmable Shape-Shifting Micelles. *Angew. Chem. Int. Ed.* **2010**, *49*, 5076-5080.
- 16 Qi, H.; Zhou, T.; Mei, S.; Chen, X.; Li, C. Y. Responsive Shape Change of Sub-5 nm Thin, Janus Polymer Nanoplates. *ACS Macro Lett.* **2016**, *5*, 651-655.
- 17 Singamaneni, S.; McConney, M. E.; Tsukruk, V. V. Swelling-Induced Folding in Confined Nanoscale Responsive Polymer Gels. *ACS Nano* **2010**, *4*, 2327-2337.
- 18 Kozlovskaya, V.; Higgins, W.; Chen, J.; Kharlampieva, E. Shape Switching of Hollow Layer-by-Layer Hydrogel Microcontainers. *Chem. Commun.* **2011**, *47*, 8352-8354.
- 19 Kozlovskaya, V.; Wang, Y.; Higgins, W.; Chen, J.; Chen, Y.; Kharlampieva, E. pH-Triggered Shape Response of Cubical Ultrathin Hydrogel Capsules. *Soft Matter* **2012**, *8*, 9828-9839.
- 20 Tian, Z.; Zhang, L.; Fang, Y.; Xu, B.; Tang, S.; Hu, N.; An, Z.; Chen, Z.; Mei, Y. Deterministic Self-Rolling of Ultrathin Nanocrystalline Diamond Nanomembranes for 3D Tubular/Helical Architecture. *Adv. Mater.* **2017**, *29*, 1604572.
- 21 Cho, J. H.; James, T.; Gracias, D. H. Curving Nanostructures Using Extrinsic Stress. *Adv. Mater.* **2010**, *22*, 2320-2324.
- 22 Xu, W.; Qin, Z.; Chen, C.; Kwag, H. R.; Ma, Q.; Sarkar, A.; Buehler, M. J.; Gracias, D. H. Ultrathin Thermoresponsive Self-Folding 3D Graphene. *Sci. Adv.* **2017**, *3*, e1701084.
- 23 Shim, T. S.; Estephan, Z. G.; Qian, Z.; Prosser, J. H.; Lee, S. Y.; Chenoweth, D. M.; Lee, D.; Park, S.; Crocker, J. C. Shape Change Thin Films Powered by DNA Hybridization. *Nat. Nanotechnol.* **2017**, *12*, 41-47.
- 24 Frolov, V. A.; Shnyrova, A. V.; Zimmerberg, J. Lipid Polymorphisms and Membrane Shape. *Cold Spring Harbor Perspect. Biol.* **2011**, *3*, a004747.
- 25 Rahimi, M.; Regan, D.; Arroyo, M.; Subramaniam, A. B.; Stone, H. A.; Staykova, M. Shape Transformations of Lipid Bilayers Following Rapid Cholesterol Uptake. *Biophys. J.* **2016**, *111*, 2651-2657.

26 Sato, Y.; Hiratsuka, Y.; Kawamata, I.; Murata, S.; Shin-ichiro, M. N. Micrometer-Sized Molecular Robot Changes Its Shape in Response to Signal Molecules. *Sci. Rob.* **2017**, 2, eaal3735.

27 van Oers, M. C.; Rutjes, F. P.; van Hest, J. C. Tubular Polymersomes: A Cross-Linker-Induced Shape Transformation. *J. Am. Chem. Soc.* **2013**, 135, 16308-16311.

28 Yan, Q.; Zhao, Y. Polymeric Microtubules That Breathe: CO₂-Driven Polymer Controlled-Self-Assembly and Shape Transformation. *Angew. Chem. Int. Ed.* **2013**, 52, 9948-9951.

29 Grubbs, R. B.; Sun, Z. Shape-Changing Polymer Assemblies. *Chem. Soc. Rev.* **2013**, 42, 7436-7445.

30 Che, H.; van Hest, J. C. Stimuli-Responsive Polymersomes and Nanoreactors. *J. Mater. Chem. B* **2016**, 4, 4632-4647.

31 Xu, W.; Ledin, P. A.; Shevchenko, V. V.; Tsukruk, V. V. Architecture, Assembly, and Emerging Applications of Branched Functional Polyelectrolytes and Poly(ionic liquid)s. *ACS Appl. Mater. Interfaces* **2015**, 7, 12570-12596.

32 Ye, C.; Nikolov, S. V.; Calabrese, R.; Dindar, A.; Alexeev, A.; Kippelen, B.; Kaplan, D. L.; Tsukruk, V. V. Self-(Un)rolling Biopolymer Microstructures: Rings, Tubules, and Helical Tubules from the Same Material. *Angew. Chem. Int. Ed.* **2015**, 127, 8610-8613.

33 Gohy, J. F.; Zhao, Y. Photo-Responsive Block Copolymer Micelles: Design and Behavior. *Chem. Soc. Rev.* **2013**, 42, 7117-7129.

34 Martin, N.; Sharma, K. P.; Harniman, R. L.; Richardson, R. M.; Hutchings, R. J.; Alibhai, D.; Li, M.; Mann, S. Light-Induced Dynamic Shaping and Self-Division of Multipodal Polyelectrolyte-Surfactant Microarchitectures via Azobenzene Photomechanics. *Sci. Rep.* **2017**, 7, 41327.

35 Kozlovskaya, V.; Alexander, J. F.; Wang, Y.; Kuncewicz, T.; Liu, X.; Godin, B.; Kharlampieva, E. Internalization of Red Blood Cell-Mimicking Hydrogel Capsules with pH-Triggered Shape Responses. *ACS Nano* **2014**, 8, 5725-5737.

36 Zhao, Q.; Qi, H. J.; Xie, T. Recent Progress in Shape Memory Polymer: New Behavior, Enabling Materials, and Mechanistic Understanding. *Prog. Polym. Sci.* **2015**, 49, 79-120.

37 Brini, E.; Algaer, E. A.; Ganguly, P.; Li, C.; Rodríguez-Ropero, F.; van der Vegt, N. F. Systematic Coarse-Graining Methods for Soft Matter Simulations—A Review. *Soft Matter* **2013**, 9, 2108-2119.

38 Huang, Q.; Hu, S.; Zhuang, J.; Wang, X. MoO_{3-x}-Based Hybrids with Tunable Localized Surface Plasmon Resonances: Chemical Oxidation Driving Transformation from Ultrathin Nanosheets to Nanotubes. *Chem. Eur. J.* **2012**, 18, 15283-15287.

39 Lin, X.; Fang, Y.; Zhu, L.; Zhang, J.; Huang, G.; Wang, J.; Mei, Y. Self-Rolling of Oxide Nanomembranes and Resonance Coupling in Tubular Optical Microcavity. *Adv. Opt. Mater.* **2016**, 4, 936-942.

40 Cho, J. H.; Keung, M. D.; Verellen, N.; Lagae, L.; Moshchalkov, V. V.; Van Dorpe, P.; Gracias, D. H. Nanoscale Origami for 3D Optics. *Small* **2011**, 7, 1943-1948.

41 Huang, M.; Cavallo, F.; Liu, F.; Lagally, M. G. Nanomechanical Architecture of Semiconductor Nanomembranes. *Nanoscale* **2011**, 3, 96-120.

42 Chalapat, K.; Chekurov, N.; Jiang, H.; Li, J.; Parviz, B.; Paraoanu, G. S. Self-Organized Origami Structures via Ion-Induced Plastic Strain. *Adv. Mater.* **2013**, 25, 91-95.

43 Xu, S.; Yan, Z.; Jang, K. I.; Huang, W.; Fu, H.; Kim, J.; Wei, Z.; Flavin, M.; McCracken, J.; Wang, R.; Badea, A.; Liu, Y.; Xiao, D.; Zhou, G.; Lee, J.; Chung, H. U.; Cheng, H.; Ren, W.; Banks, A.; Li, X.; Paik, U.; Nuzzo, R. G.; Huang, Y.; Zhang, Y.; Rogers, J. A. Assembly of Micro/Nanomaterials into Complex, Three-Dimensional Architectures by Compressive Buckling. *Science* **2015**, 347, 154-159.

44 Kosynkin, D. V.; Higginbotham, A. L.; Sinitskii, A.; Lomeda, J. R.; Dimiev, A.; Price, B. K.; Tour, J. M. Longitudinal Unzipping of Carbon Nanotubes to Form Graphene Nanoribbons. *Nature* **2009**, 458, 872-876.

45 Kelby, T. S.; Wang, M.; Huck, W. T. Controlled Folding of 2D Au–Polymer Brush Composites into 3D Microstructures. *Adv. Funct. Mater.* **2011**, 21, 652-657.

46 Ionov, L. Hydrogel-Based Actuators: Possibilities and Limitations. *Mater. Today* **2014**, 17, 494-503.

47 Wang, H.; Zhen, H.; Li, S.; Jing, Y.; Huang, G.; Mei, Y.; Lu, W. Self-Rolling and Light-Trapping in Flexible Quantum Well-Embedded Nanomembranes for Wide-Angle Infrared Photodetectors. *Sci. Adv.* **2016**, 2, e1600027.

48 Gallon, E.; Matini, T.; Sasso, L.; Mantovani, G.; Armiñan de Benito, A.; Sanchis, J.; Caliceti, P.; Alexander, C.; Vicent, M. J.; Salmaso, S. Triblock Copolymer Nanovesicles for pH-Responsive Targeted Delivery and Controlled Release of siRNA to Cancer Cells. *Biomacromolecules* **2015**, 16, 1924-1937.